The Holocene fluvial history of the Tremithos river (south central Cyprus) and its linkage to archaeological records

Matthieu Ghilardi[1], Stéphane Cordier[2], Jean-Michel Carozza[3], David Psomiadis[1], Jean Guilaine[4], Zomenia Zomeni[5], François Demory[1], Doriane Delanghe-Sabatier[1], Marc-Antoine Vella[1], Guenaëlle Bony[1], Christophe Morhange[1,6]

[1]CNRS UMR 7330 CEREGE, Aix-en-Provence CEDEX, France, [2]Département de Géographie et UMR 8591 CNRS, Université Paris 1-Université Paris Est Créteil, Créteil Cedex, France, [3]Département de Géographie, 3 Rue de l'Argonne, 67000 Strasbourg, France, [4]Collège de France, Paris, France, [5]Cyprus Geological Survey, Nicosia, Cyprus, [6]Aix-Marseille Université, Institut Universitaire de France, France

This study aims to reconstruct the Holocene fluvial history of the Tremithos river, south central Cyprus and examine linkages to regional and local archaeological records. Three stratigraphic profiles (Sp1, Sp2 and Sp3) located in the lower valley have been investigated using sedimentology and magnetic parameters. The ^{14}C dating of 10 samples reveals mid-Holocene ages for Sp1 and Sp2, while the upper most part of Sp3 can be attributed to the early to mid-Holocene. Two main phases of vertical accretion have been recognised: the first, recorded in the lower most part of Sp3, could not be dated but might relate to the late Glacial period. It is not associated with any archaeological artefacts. The second, recorded in all profiles, dating from ca. 5000 to ca. cal 2800 BC, spans the Late Neolithic Sotira (cal 4800/4000 BC) and Late Chalcolithic (cal 2900–2500 BC) cultures. The sediments of Sp1 and Sp2 are up to 8–10 m thick and mainly composed of fine material. However, an intercalated phase of coarse sediment has been identified at the beginning of the third millennium BC, indicating a sudden change in river dynamics, potentially associated with the 5.2 ka rapid climate change regional event. Typical mid-Chalcolithic (ca. cal 3300–3050 BC) ceramics found in a palaeosol in Sp2 indicate for the first time human occupation of the Tremithos river terraces. Two other palaeosols have also been recognised in Sp3 and radiocarbon dated to ca. cal 5600–4100 BC and ca. cal 2900–2600 BC, respectively. These results make it possible to propose a palaeogeographic reconstruction of the Holocene evolution in the Tremithos valley and to make a preliminary assessment of the relative roles of tectonics, climate and anthropogenic forcing.

Keywords: Cyprus, Holocene, Chalcolithic, Fluvial terraces, sedimentology, Tremithos river

Introduction

The factors responsible for alluvial landscape evolution in the eastern Mediterranean valleys since the Last Glacial maximum, in particular disentangling natural and anthropogenic factors, have been a matter of debate since the late 1960s (Vita-Finzi 1969; Bintliff 2002; Butzer 2005; Fuchs 2007; Devillers 2008). Many authors have suggested that alluvial terraces represent reliable archives for assessing the respective roles of tectonic, climatic and anthropogenic controls on landscape evolution (e.g. Brown 1985; Bridgland and Westaway 2008; De Moor *et al.* 2008; Notebaert and Verstraeten 2010; Dusar *et al.* 2011; Wolf *et al.* 2014). Recently, geoarchaeological approaches, combining several proxies, have highlighted the consequences of human activity on Holocene fluvial landscapes in the eastern Mediterranean (Dusar *et al.* 2011), and in particular in the Aegean area (Lespez 2003; Unkel *et al.* 2014). On the island of Cyprus, despite the presence of numerous incised valleys, which formed during Late Cenozoic and Quaternary as a response to tectonic uplift (Dalongeville *et al.* 2000; Kinnaird *et al.* 2011), permanent streams are lacking because of the semi-arid (Mediterranean) to arid climate (Grove 1977; Devillers 2005). Vertically accreted alluvial deposits are therefore rare (Butzer and Harris 2007), making the reconstruction of Holocene palaeoenvironments challenging. Few places (mainly in the

Correspondence to: Matthieu Ghilardi, CNRS UMR 7330 CEREGE, Europôle de l'Arbois, BP 80 13545, Aix-en-Provence CEDEX 04, France. Email: ghilardi@cerege.fr

DOI 10.1179/1749631414Y.0000000057

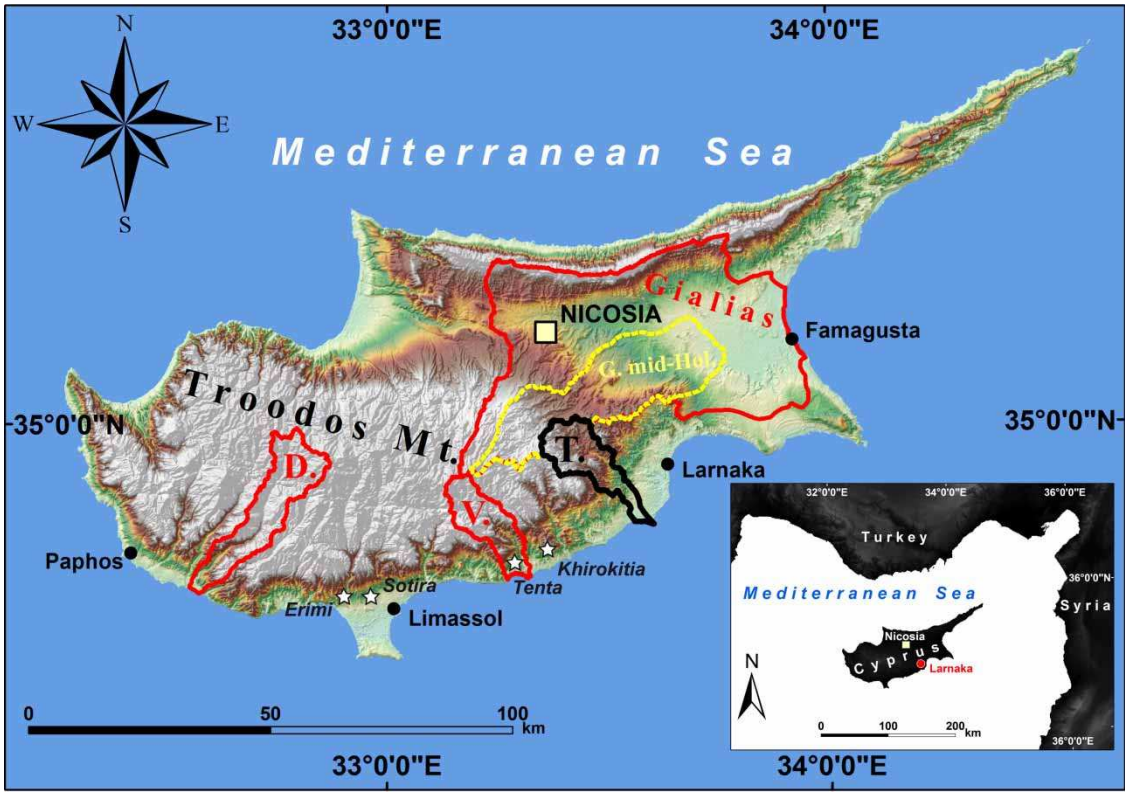

Figure 1 Location map of the Tremithos (T.) drainage basin. D.: Dhiarizos catchment; V.: Vassilikos catchment; G. or mid-Hol.: Gialias catchment configuration during early to mid-Holocene (after Devillers, 2005). The white stars show the location of major archaeological sites mentioned in this paper (Erimi, Sotira, Tenta and Khirokitia).

Dhiarizos, Gialias and Vassilikos catchments, Fig. 1) have been investigated in a way that combines Holocene alluvial stratigraphy and settlement history (Gomez 1987; Deckers 2002, 2005; Devillers 2005, 2008; Butzer and Harris 2007; Noller 2009). The archaeological periods covered by this research, however, mainly comprise the Bronze Age and medieval times with less concern given to earlier periods (e.g. Neolithic and Chalcolithic times). This is in spite of the fact for the oldest known Neolithic sites of the Mediterranean occur on Cyprus and most of such settlements are intimately connected to river valleys (e.g. the Koirokitia and Tenta aceramic Neolithic sites, Fig. 1), being located on rocky promontories overhanging the floodplains of dried-up rivers (Guilaine 2011; Knapp 2013). A key issue is therefore the role played by the configuration of the fluvial landscape in the settlement strategy of the human societies, as well as the anthropogenic forcing on alluvial systems during crucial periods for the settlement history of Cyprus such as Neolithic and Chalcolithic.

The Tremithos is among the Cypriot valleys that have not previously been investigated for geoarchaeological purposes. Archaeological surveys and excavation were conducted during the late 1970s (Gifford 1978) and the early 1980s (Baudou and Engelmark 1983; Baudou *et al.* 1985). Finds of flints and cherts, attributed to Upper Palaeolithic (Baudou and Engelmark 1983), were found embedded within the alluvial sediments, providing evidence for early human occupation. However, the nature of the Palaeolithic occupation is still a matter of debate (Karageorghis 1982; Simmons 1999), and the palaeoenvironmental context for these findings remains unclear. The aim of this paper is to present geoarchaeological investigations conducted in the lower Tremithos valley. Our research was primarily based on the study of the alluvial landforms and deposits. However, the recognition of archaeological records within the alluvial sequence along with radiocarbon dating has made it possible to establish linkages between the Holocene alluvial history of the Tremithos catchment and local and regional archaeological records.

Geological Settings and Geomorphology of the Tremithos Catchment

Cyprus is the third largest Mediterranean island, spanning an area of ca. 9250 km^2. It is characterised by asymmetric relief: a high western part, culminating in the upper Cretaceous ophiolitic Troodos massif (1950 m at Mount Olympus, Fig. 1), and an eastern part where the relief is generally smoother and lower. The Troodos ophiolitic complex and associated autochthonous sediments have been gradually uplifted from below sea level to their present elevation during periods of rapid but spasmodic uplift, which took place throughout the Middle to Upper Cenozoic

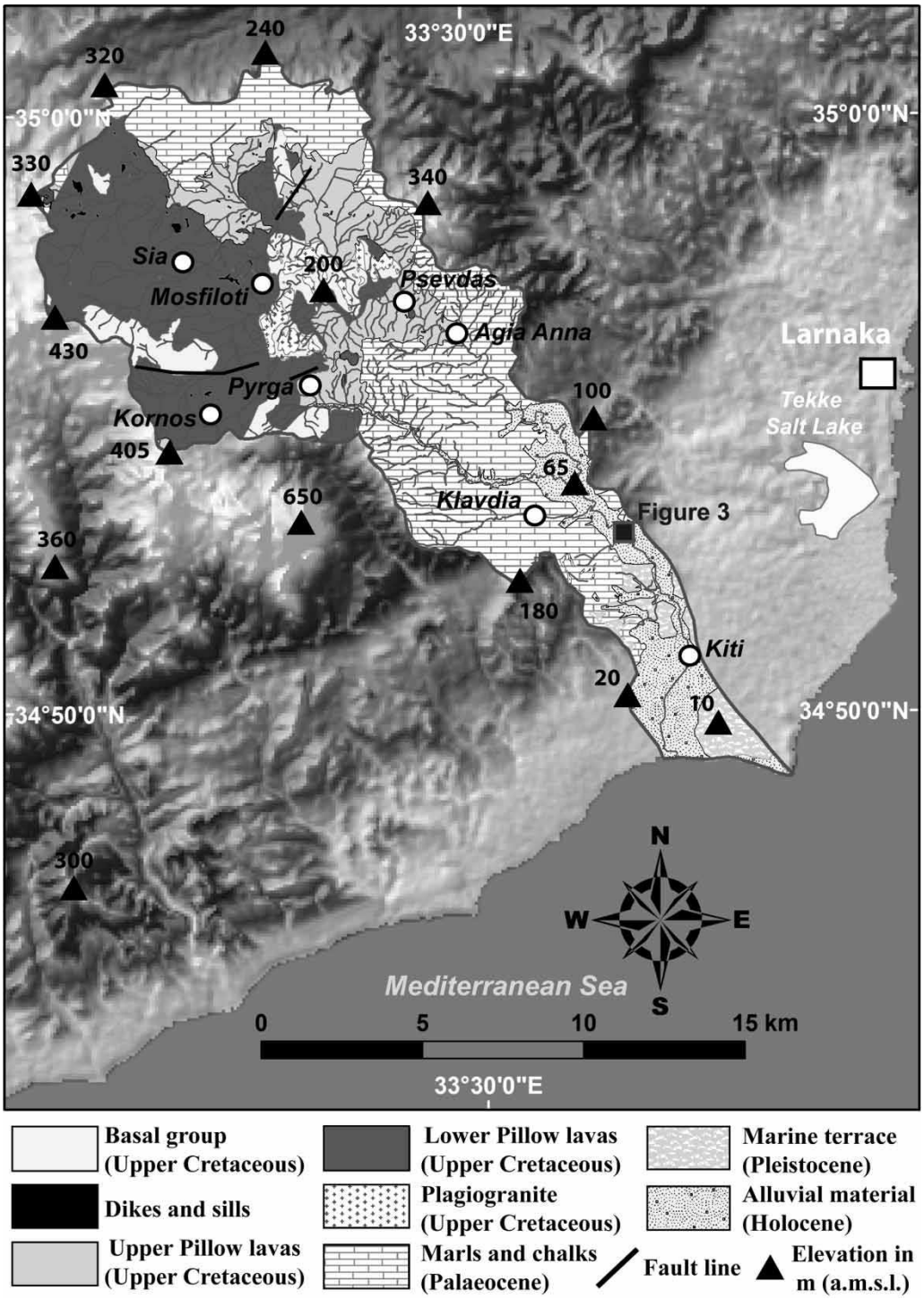

Figure 2 Geological map of the Tremithos catchment and location of the study area. Data were provided by the Geological Survey of Cyprus. The elevations are derived from the SRTM – *Shuttle Radar Topography Mission* – data (version 3).

(Poole *et al.* 1990; Vita-Finzi 1993; Kinnaird *et al.* 2011). The Tremithos river, also called *Tetius Flavius* by the 2nd century AD Alexandrian geographer Ptolemy (Oberhummer 1903), is located in the southern part of the island (Fig. 1). Its catchment covers an area of ca. 170 km^2 and the total length of the river does not exceed 25 km (Figs. 1 and 2). The western part of the catchment (up to 450 m in elevation) is composed of Upper Cretaceous igneous rocks (mainly pillow lava, dykes and basalts, Fig. 2). Copper ore is known to have been mined in this area for several centuries though its exploitation is likely to have occurred over several thousand years. In the northern and central parts of the catchment, Palaeocene–Miocene marls and limestones predominate. The middle sections of the Tremithos valley and its tributaries are deeply incised, especially in the vicinity of Agia Anna (Fig. 2) where thick colluvial deposits overlie the bedrock. Further downstream, in the area of Klavdia-Kiti, the lower Tremithos occupies a lowland area in which sedimentation has predominated, leading to the formation of a large alluvial

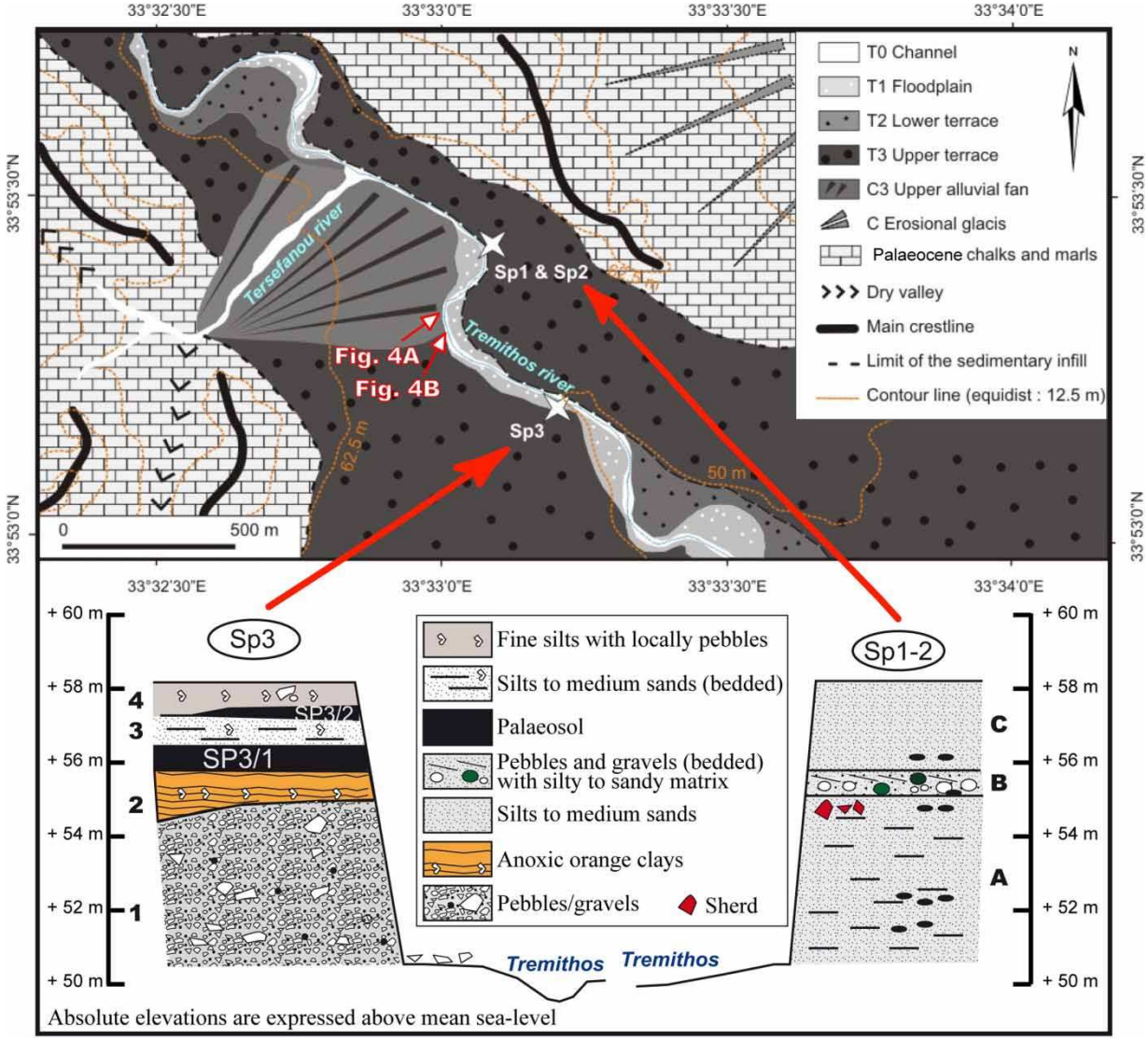

Figure 3 Geomorphological map of the Lower Tremithos valley (top) and synthetic description of the studied profiles (bottom). The stars indicate the location of the stratigraphic profiles (Sp1, Sp2 and Sp3) studied in this paper.

fan ending in the sea 3 km south of Kiti (Gifford 1978). Previous research (Bagnall 1960; Gifford 1978) recognised two fluvial terraces (T3 and T2, Fig. 3) in the middle and lower Tremithos valley between Agia Anna and Klavdia (Figs. 2 and 3). The upper terrace T3 (Figs. 3 and 4A and B) is located ca. 8–10 m above the present-day riverbed and may be correlated with the surface of the alluvial fan C3 (Fig. 4A) developed in the lower valley. In contrast, the lower terrace (T2, Fig. 4A) deposits are preserved within a channel cut into the upper terrace. This palaeochannel is only ~3 m above the present-day riverbed (T1, Fig. 4) and is filled with muddy sands, with a soil horizon developed on its upper surface. Little is known about the sedimentation rates of the Tremithos river. Morhange *et al.* (2000) and Bony (2013) only suggested that the Tremithos river brought a significant quantity of sediment (mostly pebbles) to the coast during Hellenistic to Roman times (ca. cal 300 BC to cal 200 AD), leading to the formation of a coastal barrier (spit) in the vicinity of Ancient Kition (the modern city of Larnaka, Fig. 2).

Regional and Local Holocene Environmental Change

Alluvial Response to Holocene Climate Change and Human Activity in the Eastern Mediterranean

In the wider eastern Mediterranean, significant changes in climate and fluvial dynamics are reported during the Holocene (Mayewski *et al.* 2004; Finné *et al.* 2011). Prior to ca. 4000 BC the eastern Mediterranean is considered as being wetter than today (Roberts *et al.* 2011). Following this, the mid-Holocene climatic shift was typically initiated by a decrease in wetness during the fourth millennium BC (Roberts *et al.* 2004, 2011), which included a strong but rather short-lived drought peak at around 5.2–5.1 ka BP (Roberts *et al.* 2011), regionally well-recorded in the Soreq Cave isotope record (Bar-

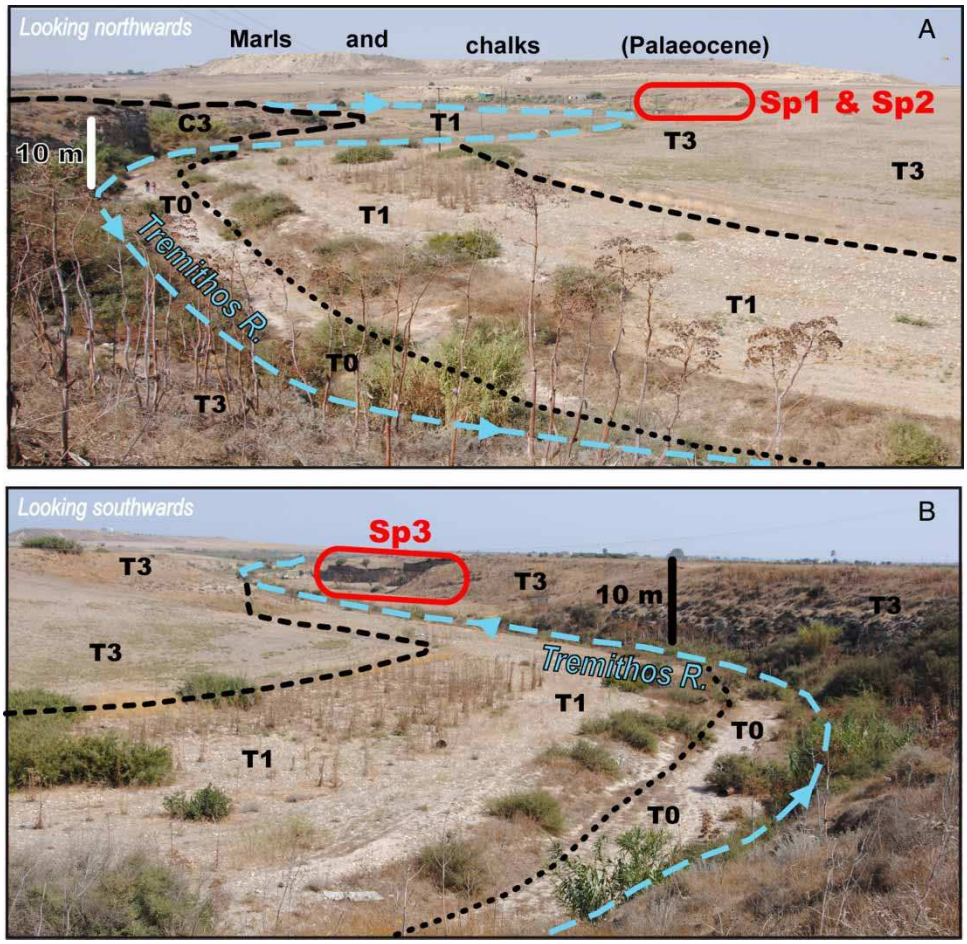

Figure 4 Views of the Sp1, Sp2 and Sp3 profiles. (A) shows the Tremithos valley looking northwards in direction of the Sp1-2 profiles. (B) is a view of the Tremithos valley looking southwards in the direction of the Sp3 profile.

Matthews *et al.* 1997) and in the Lake Van record in Turkey (Lemcke and Sturm 1997). Some authors therefore consider that the period cal 5300–5000 BP (ca. cal 3300–3000 BC) is one of the driest experienced in the Mediterranean (Marchetto *et al.* 2008; Noti *et al.* 2009). In the review by Robinson *et al.* (2006), a subsequent mid-Holocene wet period is suggested around cal 3000 BC in the Levant, following drier conditions in the later mid-Holocene.

Alluvial dynamics were apparently enhanced by wetter conditions during the Holocene (Dusar *et al.* 2011). However, it has been shown (Butzer 2005) that fluvial evolution was also influenced from the mid-Holocene onwards by anthropogenic activity (in particular related to changes in land use). Research on fluvial systems from the eastern Mediterranean area suggests that wetter periods frequently produce continuous sedimentation, while incision and flooding seem to occur during drier periods and/or climate transitions. For example in southern Anatolia (which is the most well-documented and the closest area to Cyprus), three periods of floodplain sedimentation, related to humid conditions which have been recorded (at cal 7000, 3500 and 2000 BC), were followed by phases of vertical incision (Collins *et al.* 2005). In the Lake Tuz area (central Turkey), two major periods of alluvial fan formation associated with a relatively wet climate have been recognised, a major one between cal 5000 and 3500 BC and a minor one around cal 2300 BC (Kashima 2002).

Holocene Fluvial History of Cyprus: A Combination of Natural and Human Influences?

The influence of Holocene climatic changes and human occupation on river systems in Cyprus have been little studied (Butzer and Harris 2007) and remain subject to debate (Gomez 1987; Devillers and Morhange 2011). It is worth noting that alluvial archives are mainly concentrated in the southern valleys of the island. The first palaeoenvironmental research (Gomez 1987, 2003) was performed in the lower Vassilikos valley (located in southern Cyprus, 20 km east of Limassol, Fig. 1). Several alluvial terraces were recognised, providing evidence for significant alluviation during Aceramic Neolithic times (ca. cal 5800–5250 BC). However, the chronology was based on archaeological evidence, with only a few radiocarbon ages. In addition, there was no specific focus on the evolution of the alluvial system, as the main aim of the research was the recognition of the

'older and younger' fills (Vita-Finzi 1969). More recently, the alluvial formations of the Dhiarizos River (ca. 15 km east of Paphos, Fig. 1) have been intensively studied (Deckers 2002, 2003, 2005; Deckers *et al.* 2005) particularly for the post Roman period. These studies suggested that a braided river system may have been active from ca. cal 11,000 to 5000 BC, leading to the accumulation of coarse sediments (gravels, coarse sands, etc.) in the lower valley. However, the lack of absolute dating from the early to mid-Holocene sediments prevented the accurate dating of the times of deposition and incision. The most complete reconstruction of fluvial history in Cyprus focused on the Gialias catchment located in the eastern part of the island, near the city of Famagusta (Fig. 1). In this area, research has led to the recognition of several periods of Holocene alluviation separated by incision events (Devillers *et al.* 2002; Devillers 2005, 2008). Four palaeosol levels were identified within the fluvial deposits and dated respectively to ca. cal 9300, 7400, 4400 and 3800 BC (Devillers 2008). These palaeosols were attributed to wetter conditions (Devillers and Morhange 2011). They suggest that alluviation occurred periodically between ca. cal 9000 and 3000 BC in the Gialias catchment, which is consistent with the assumptions made from the Dhiarizos (Deckers 2003) and lower Vassilikos valleys (Gomez 1987). The 12 m of vertical accretion was followed by a major incision (approximately 6–8 m) dated ca. cal 3000–1900 BC (Devillers and Morhange 2011). The research on the Gialias is unrivalled at a catchment scale and crucial in showing that, in contrast with the lack of permanent rivers today, continuous fluvial activity occurred on Cyprus during the early to mid-Holocene. However, the results from the Gialias did not allow identification of regional/local climate events or human controls on the sedimentation process. Furthermore, the role of tectonics as a driver was insufficiently included in explanations of the timing of sediment deposition/incision since Upper Pleistocene.

Prehistoric Human Occupation

Human occupation of Cyprus is characterised by intense settlement development between the early Neolithic and Chalcolithic periods (Guilaine *et al.* 1999; Butzer and Harris 2007; Guilaine 2011). The first main period of settlement corresponds with the Khirokitia culture (see Fig. 1 for site locations). An important hiatus in terms of human occupation then took place dated to the second part of the 7th millennium BC (Weninger *et al.* 2006), and/or the first half of the 6th millennium BC (Le Brun *et al.* 1987). The second half of the 6th millennium BC is characterised by the first spread of grey ware ceramics, although evidence for human occupation remains scarce (Dikaios 1962). The Late Neolithic (cal 4800/4000 BC) is associated with the development of the so called Sotira culture and increasing human occupation in the whole island. Archaeological surveys have revealed that typical Sotira buildings consisted of rectangular houses with agricultural practices based on cereal cultivation and husbandry (Guilaine 2011). The Sotira culture lasted until ca. cal 3800 BC. Less information is available for the subsequent Chalcolithic period (from the early phases of the 4th millennium BC to cal 3500 BC), in particular since building strategies often used perishable materials (wood). The Middle Chalcolithic era (3500–2900 BC) is, however, considered as a major period of human occupation in the southern part of the island, with Erimi as the type locality. It is also marked by the first evidence of metal work (copper) and the exploitation of picrolite for construction.

The archaeology of the Tremithos catchment is poorly documented: an archaeological survey conducted in 1980 (Baudou and Engelmark 1983) focused on six sites in the area of Aghia Anna (Fig. 2). This study found chert tools, similar to those observed for the first phase of Khirokitia and roughly dated to ca. cal 7000 BC (Le Brun *et al.* 1987). However, no settlements were found. Furthermore, the lithics at this site appear to have been reworked and caution should therefore be exercised in relation to their stratigraphic position (Todd 1987; Button 2010). No other Neolithic or Chalcolithic sites had been firmly identified in the Tremithos catchment until the present study.

Methods

Site Selection and Sampling Strategy

Field survey performed in the Tremithos catchment allowed the recognition of three natural sections (Sp1, Sp2 and Sp3, Figs. 3 and 4A and B) preserved in a small section of the lower valley, 3 km southeast of the modern city of Klavdia (Figs. 2, 4A, B and 5). Due to its thickness (up to 10 m) and the diversity of alluvial facies, the deposits of the upper terrace T3 (Fig. 3) were chosen for detailed investigation.

Field methods consisted of (1) collecting 40 surface samples of the fluvial sediments (sandy fraction below 2 mm) found in the river bed of the Tremithos and its tributaries from the whole catchment (Fig. 6) and (2) sampling of the three stratigraphic profiles. All samples have been studied for grain-size analysis and magnetic susceptibility measurements. The latter allows the concentration of magnetic particles to be evaluated (Dearing 1999), which proved useful in identifying palaeosols and distinguishing different sediment sources (Smith, 1985; Walden and Slattery 1993; Oldfield 2007; Ghilardi *et al.* 2008; Ghilardi and Boraik 2011). Ten Accelerator Mass

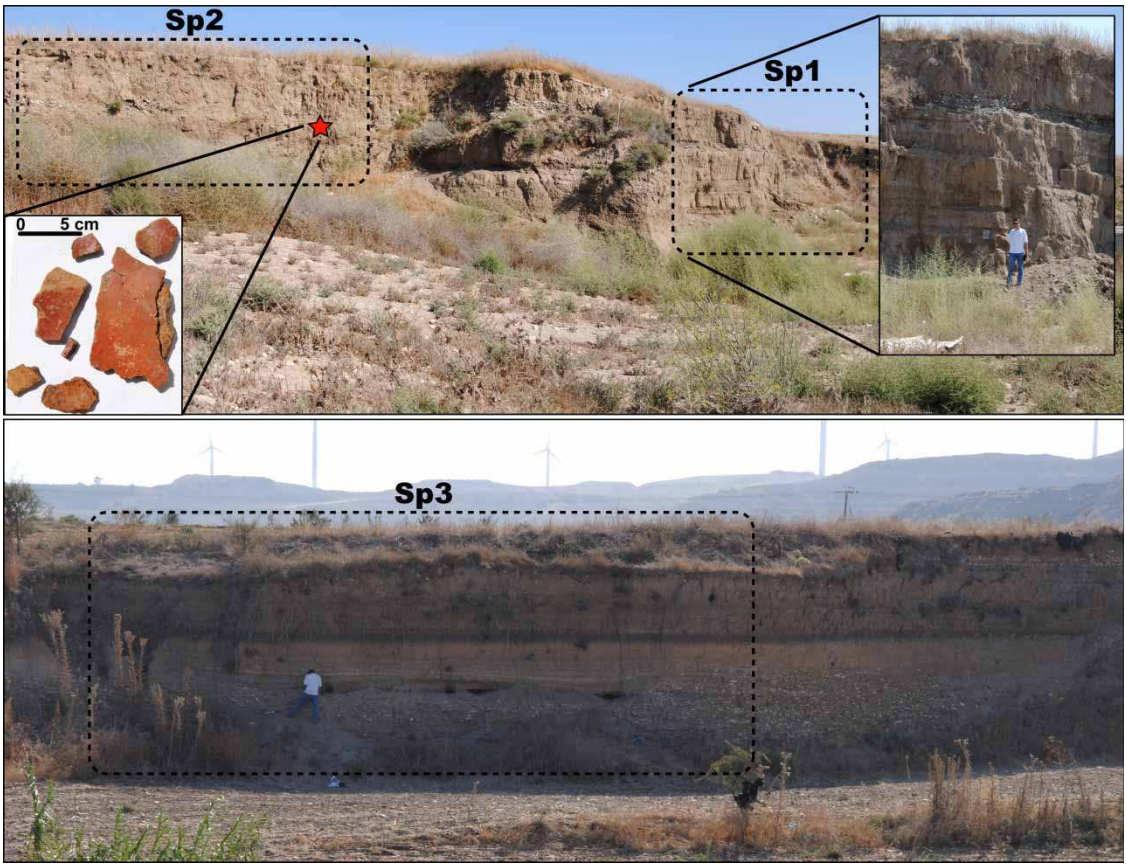

Figure 5 The Sp1 and Sp2 profiles (top) and of Sp3 (bottom). Refer to Fig. 3 for the location of the sections.

Spectrometry (AMS) radiocarbon dates were obtained from the Sp1, Sp2 and Sp3 profiles.

Magnetic Susceptibility Measurements

A total of 54 samples were collected from sediments exposed both in the main profiles under study and inside the channels of the Tremithos river tributaries. They were placed in 8 cm^3 plastic boxes, dried and weighed. Only soft material derived from the erosion of the bedrock was sampled (fraction below 2 mm) at a maximum depth of 20 cm below the surface (see also Ghilardi *et al.* 2008).

Magnetic susceptibility measurements were performed at the Centre Européen de Recherche et d'Enseignement des Géosciences de l'Environnement (CEREGE) using a MFK1 magnetic susceptibility metre (Agico, Brno, Czech Republic)), which has a sensitivity of 3×10^{-8} SI at 976 Hz. The magnetic susceptibility values were divided by the density of the dried samples in order to derive mass-specific susceptibilities (χ). This measurement includes the contribution of diamagnetic, paramagnetic, ferromagnetic and imperfect antiferromagnetic particles, but high values mostly reflect ferromagnetic particle concentration. In addition to low-field magnetic susceptibility, measured at the 976 Hz frequency, measurements were also performed at the 15,616 Hz frequency. Magnetic susceptibility measurements at two frequencies are used to detect ultrafine (<0.03 mm) superparamagnetic particles, which can be produced by bacteria or chemical processes during soil formation (Dearing *et al.* 1996), by firing events (Oldfield 2007; Oldfield and Crowther 2007) or derived from baked clays (pottery production, Dearing *et al.* 1996; Jordanova *et al.* 2003). The contribution of superparamagnetic particles is given by frequency-dependent susceptibility ($\chi fd_{\%}$).

LASER Grain-Size Analysis

Grain-size determinations of the magnetic susceptibility samples from Sp1, Sp2 and Sp3 were conducted at the CEREGE. They were sub-sampled in order to match the optimal obscuration windows of the laser and of the light polarisation system, between 8 and 16% and between 50 and 70%, respectively. The solution was mixed with 0.3% sodium hexametaphosphate in order to disperse the clay particles. Aliquots of 10 ml, mixed using a magnetic stirrer plate at 800 rpm, were pipetted with a reproducibility constrained at <1–2%. The grain-size distribution was measured using a Beckman Coulter LS 13 320 (Brea, California, USA) laser granulometer with a range of 0.04–2000 microns, in 132 fractions. The calculation model uses Fraunhöfer and Mie theory. This model uses water as the medium (refractive index (RI) = 1.33 at 20°C), which has a RI in the range of that of kaolinite for the solid phase (RI = 1.56), and

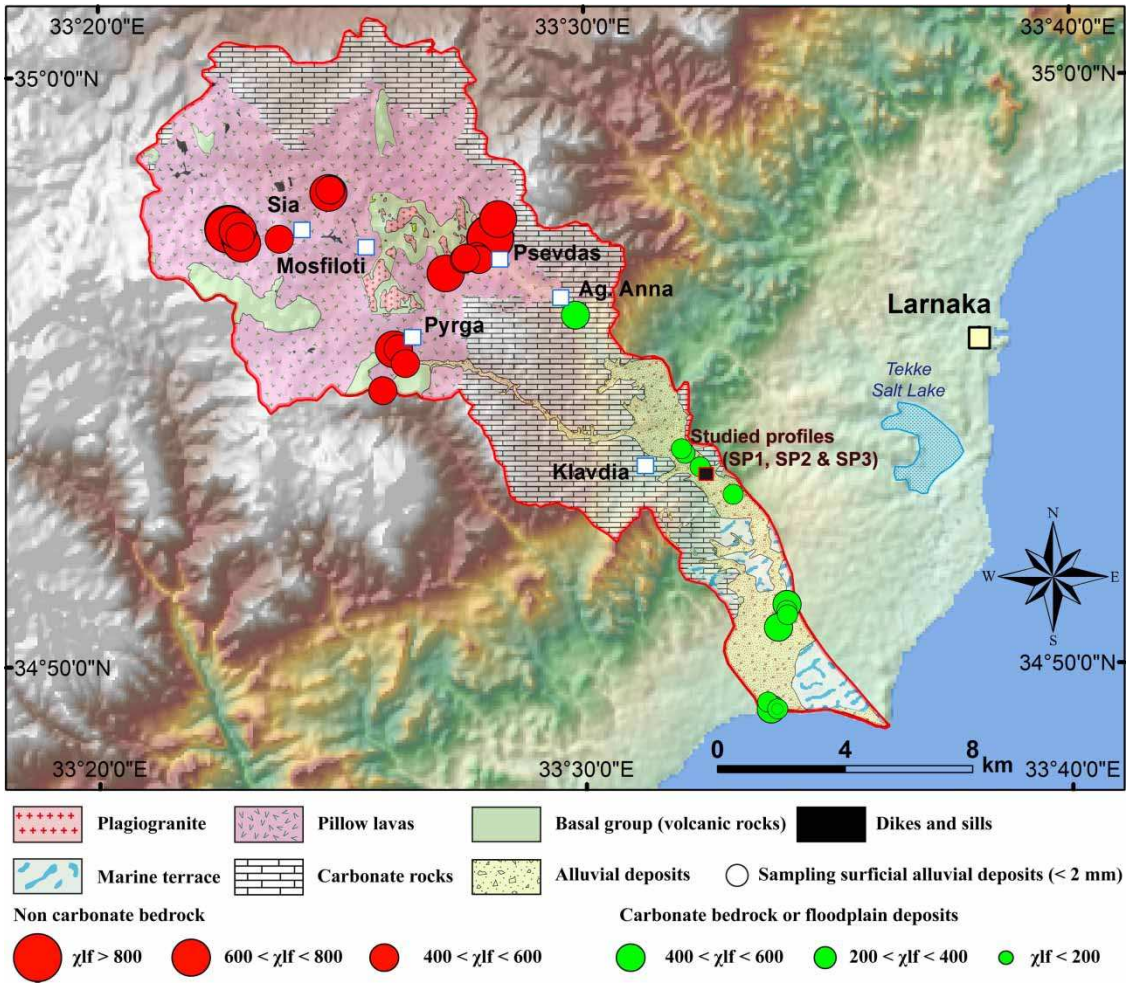

Figure 6 Magnetic susceptibility mapping of the modern alluvial sediments of the Tremithos catchment. The values correspond to the low field mass specific susceptibility (see Table 2 for complete results). Only the fraction below 2 mm was sampled in order to compare the results with those from profiles Sp1, Sp2 and Sp3.

absorption coefficients of 0.15 for the 780-nm laser wave length and 0.2 for the polarised wavelengths (Buurman *et al.* 1996). Each sample was analysed 6 times for 90 seconds. The result is an average of the five last passages as small bubbles can perturb the integration phase after the rinsing phase.

AMS Radiocarbon Dating

The chronostratigraphy of profiles Sp1, Sp2 and Sp3 was determined using a series of 10 AMS radiocarbon determinations performed on millimetre-sized charcoal and diffuse organic matter samples (Table 1). The ^{14}C ages were calibrated using the CALIB 7.0.2 software and the IntCal13 calibration curve (Bronk Ramsey 2009; Reimer *et al.* 2013; Table 1). Ages are expressed as calibrated calendar years (cal BC). In order to obtain an independent age control, four samples for luminescence dating were also taken from the main sediment body. However, due to the paucity of quartz and K-rich feldspars and to the

Table 1 Radiocarbon dates

Profile and sample reference	Elevation (in m)	Material	BP	Error±	Cal. 2σ	Lab. reference
Sp1 Charcoal 1	+544	Charcoal	4510	40	3361–3091 BC	Poz-44096
Sp1 Charcoal 2	+52	Charcoal	5290	40	4239–3992 BC	Poz-44098
Sp1 Charcoal 3	+51.8	Charcoal	5270	40	4232–3986 BC	Poz-44099
Sp1 Charcoal 4	+51.4	Charcoal	5680	50	4681–4373 BC	Poz-44097
Sp2 Charcoal 5	+56	Charcoal	4420	40	3328–2918 BC	Poz-44102
Sp2 Charcoal 6	+55.4	Charcoal	4480	35	3342–3029 BC	Poz-44101
Sp2 Charcoal 7	+55	Charcoal	4480	40	3349–3026 BC	Poz-44100
Sp3/2 Palaeosol – middle part	+57	Diffuse organic matter	4175	35	2886–2659 BC	Poz-65051
Sp3/1 Palaeosol – upper part	+56.4	Diffuse organic matter	5320	40	4262–4042 BC	Poz-65052
Sp3/1 Palaeosol – middle part	+56.2	Diffuse organic matter	6750	70	5765–5530 BC	Poz-65050

Absolute elevations refer to the World Geodetic System 84 projection datum and are expressed in m above mean sea level.

poor properties of the OSL luminescence signal, it was not possible to infer age estimates.

Results

Magnetic Susceptibility Values of the Tremithos Catchment Surface Sediments

The magnetic susceptibility values measured from the catchment surface sediments typically reflect the mineral composition of the bedrock. A contrast was thus recognised between the upper catchment (developed in the ultramafic volcanic rocks of the Sia-Pyrga-Psevdas area, see Figs. 2 and 6) and the middle and lower part of the catchment, where the Tremithos valley passes through Palaeocene carbonate rocks and Quaternary alluvium. In the upper reaches, the magnetic susceptibility signal exhibits high values, ranging from ca. 430 to $890 \times 10^{-8}\ m^3\ kg^{-1}$ (Table 2 and Fig. 6). Some peaks above $1000 \times 10^{-8}\ m^3\ kg^{-1}$ are locally recorded in the vicinity of Psevdas. χfd constantly yielded insignificant values, generally lower than 3% (with rare peaks comprise between 3 and 3.5%), reflecting a low concentration of superparamagnetic minerals. Further downstream, magnetic values gradually decrease (Table 2 and Fig. 6) due to enrichment of poorly magnetic mineral associated with the carbonate rocks (Palaeocene marls and chalks) of the Klavdia area. χ values range between 300 and $400 \times 10^{-8}\ m^3\ kg^{-1}$ and χfd is generally <2.5%, reflecting a low superparamagnetic minerals concentration. Finally, samples from the lower catchment yielded similar values as in the Psevdas area (between 350 and $500 \times 10^{-8}\ m^3\ kg^{-1}$). In the Tremithos estuary, values decrease further, to $150 \times 10^{-8}\ m^3\ kg^{-1}$, probably as a result of mixing of sediments originating from the Tremithos catchment and from longshore drift.

General Stratigraphy of Sections Sp1 and Sp2

Sections Sp1 and Sp2 are located very close to each other (Figs. 4A and 5), at the transition between the middle and the lower valley. Unfortunately, the bedrock was not observable at the base of these profiles, so the thickness of the entire sequence remains unknown. From the field observations (sedimentary and pedogenic facies analyses) and laboratory analyses, three main sedimentary units (A, B and C) have been recognised (Fig. 4A).

The basal unit A is at least 4 m thick and only exposed in the lower part of Sp1 (Figs. 5 and 7). It consists of 20–40 cm thick beds of fine to grey silty sands (80–125 μm) alternating with carbonate-rich white silty beds (20–70 μm) less than 10 cm thick. Five cycles of decreasing upwards grain-size are recorded. Medium sands have mainly been found in the lower and upper parts of the unit (modal index ranging between 120 and 180 μm). All the samples analysed had positive skewness (Table 3) with values oscillating around 1, indicating a Gaussian (right skewed) distribution, associated with well-sorted sediments. These data agree well with a low-energy fluvial origin and could be correlated to a distal to proximal alluvial plain (Fig. 7) with a well-channelised meandering pattern. The magnetic susceptibility signal shows high values, ranging between 530 and $630 \times 10^{-8}\ m^3\ kg^{-1}$ in the lower and middle parts of the unit, whereas the signal decreases in the upper part of the unit, ranging from 330 to $530 \times 10^{-8}\ m^3\ kg^{-1}$. χfd measurement yielded very constant values from the whole of unit A, ranging between 3.5 and 4%, thus reflecting a low superparamagnetic minerals concentration. Radiocarbon dating of a charcoal sampled 1.5 m above the base of Sp1 yielded an age of cal 4683–4372 BC. This age is contemporaneous with the Sotira Neolithic culture. The middle and upper parts of unit A were radiocarbon dated to ca. cal 4250–4000 BC (Late Sotira) and ca. cal 3361–3091 BC (middle Chalcolithic), respectively. It is finally worth noting the presence of pottery in the upper part of this unit (Figs. 5 and 7). Included are large-sized sherds (10 to 15 cm, Fig. 4) that show no evidence of reworking (sharp sides) and must be considered as being *in situ*. They are part of a pot, painted red monochrome, which is typical of the mid-Chalcolithic (Bolger 1988; Bolger *et al.* 1998). This finding, which is the first evidence of a chalcolithic occupation in the Tremithos valley, is in agreement with the radiocarbon ages obtained for the upper part of unit A. The artefact is associated with a palaeosol that shows higher magnetic susceptibility, with χfd values ranging between 6 and 8%. These values are significantly higher than those found in the catchment and the rest of the stratigraphic profile (generally below 4%, see section above). Such values are associated with the contribution of superparamagnetic particles, which can be attributed to human activities such as baked clays (derived from pottery sherds), firing and/or pedogenetic processes. This is consistent with the presence of numerous charcoal fragments (size of ca. 0.5 mm) in this layer that are likely to be related to anthropogenically set fires (though a natural origin cannot be completely excluded).

Unit B is found above unit A and is recorded both in Sp1 and Sp2. It is 0.5 m thick and comprises coarse black sands alternating with gravels and rounded pebbles (carbonate and volcanic rocks). The grain-size coarsening and oblique to cross-bedded stratification attest to the in-channel origin of the sequence and to important changes in the hydrodynamic conditions. This is confirmed by the sharp contact with lower unit A which provide evidence for a sudden change in fluvial dynamics rather than a progressive channel

Table 2 Magnetic susceptibility measurements of alluvial sediments (only the fraction below 2 mm in size was analysed) sampled within the Tremitos catchment basin

Site sampling	*X* (World Geodetic System 84)	*Y* (World Geodetic System 84)	χlf ($\times 10^{-8}$ m^3 kg^{-1}	χhf ($\times 10^{-8}$ m^3 kg^{-1}	χfd (%)
Mosfiloti 1	537631	3869491	608	594	2.4
Mosfiloti 2	537712	3869598	547	533	2.7
Mosfiloti 3	537690	3869574	527	512	2.7
Psevdas 1	541306	3866963	618	602	2.6
Psevdas 3	541900	3867402	424	410	3.1
Psevdas 4	541940	3867437	568	554	2.4
Psevdas 5	542273	3867487	553	542	1.9
Psevdas 6	542362	3867393	515	497	3.5
Psevdas 8	542702	3868066	1367	1345	1.6
Psevdas 9	542957	3868669	653	642	1.6
Psevdas 10	542989	3868651	364	353	3.1
Psevdas 11	543292	3868545	77	74	3.2
Psevdas 14	545375	3865652	568	553	2.6
Klavdia 1	548815	3861305	330	319	3.3
Klavdia 2	548698	3861449	301	293	2.6
Klavdia 4	549282	3860887	397	388	2.4
Klavdia 5	550323	3860029	373	363	2.6
Kiti 1	552023	3856245	363	353	2.7
Kiti 2	552008	3856384	387	375	3.0
Kiti 3	552005	3856578	574	561	2.3
Kiti 4	551742	3855861	475	464	2.4
River mouth 1	551409	3853505	370	360	2.5
River mouth 2	551514	3853290	440	432	1.8
River mouth 3	551716	3853296	357	351	1.7
River mouth 4	551712	3853295	151	147	2.8
Sia 1	534863	3868053	755	737	2.3
Sia 2	534863	3868108	562	542	3.5
Sia 3	534925	3867904	669	652	2.5
Sia 4	534790	3868311	604	590	2.3
Sia 7	534507	3868334	886	866	2.3
Sia 8	534493	3868362	890	871	2.2
Sia 10	536099	3868037	568	556	2.1
Pyrga 1	539822	3864597	599	587	2.0
Pyrga 3	539687	3864588	671	656	2.2
Pyrga 6	539343	3863285	462	450	2.6
Pyrga 8	540051	3864136	434	423	2.7

Mass-specific susceptibilities were obtained at low (976 Hz) and high (15,616 Hz) field frequencies (χlf and χhf). Refer to Fig. 5 for magnetic susceptibility mapping of the Tremithos sediments.

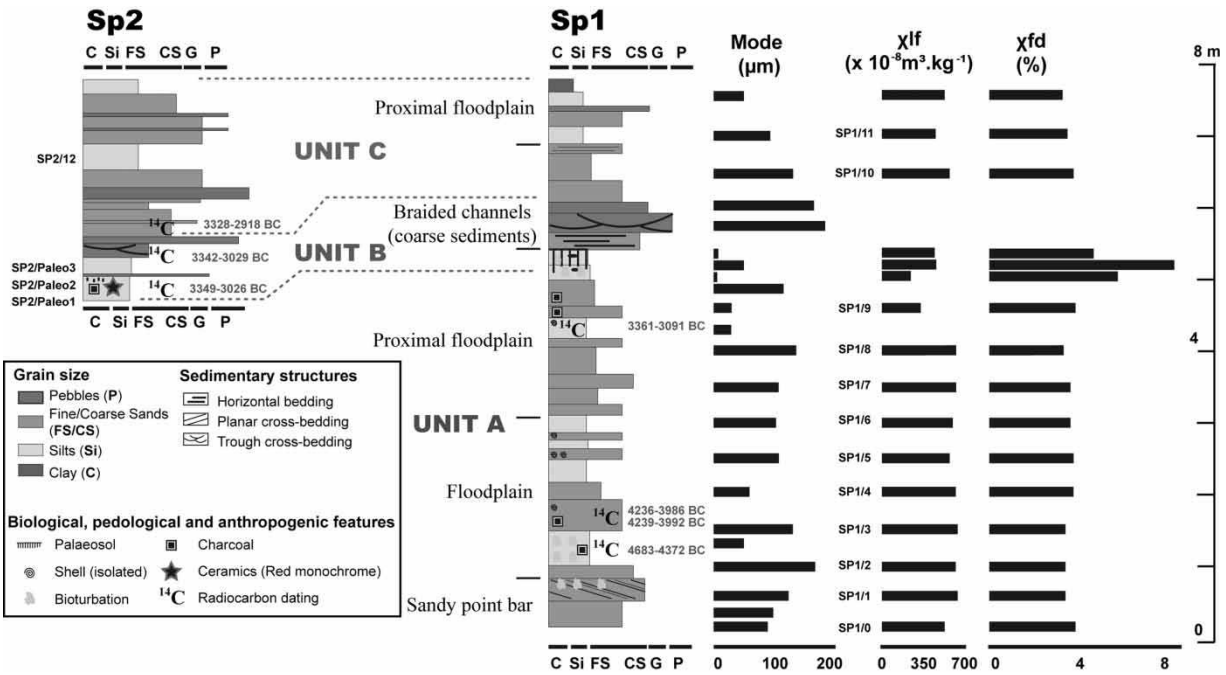

Figure 7 Schematic representation of profiles Sp1 and Sp2. The grain-size distribution is reported together with magnetic parameters (χlf and χfd). The sizes of the bars indicate the dominant textural class (refer to the legend for details). The stratigraphic positions of the radiocarbon dates (see Table 1) are also shown.

Table 3 Magnetic susceptibility measurements and LASER grain-size results obtained for samples from Sp1, Sp2 and Sp3 profiles

Profile and sample reference	Mean (μm)	Mode (μm)	Skewness	Kurtosis	<4.3 μm (%)	<20.7 μm (%)	<63.4 μm (%)	<200 μm (%)	<310 μm (%)	χlf (× 10^{-8}·m^3 kg^{-1}	χhf (× 10^{-8}·m^3 kg^{-1}	χfd (%)
Sp1/11	51.5	96.5	1.73	5.69	17.5	40.3	65.8	98.9	99.6	490	472	3.7
Sp1/10	99.3	140.1	2.15	14.25	10.8	23.8	39.9	88.7	98.1	549	530	3.5
Sp1/9	25.4	38.0	4.72	43.96	26.4	59.7	90.6	99.6	99.8	347	334	3.9
Sp1/8	68.4	140.1	1.30	1.90	17.3	37.8	58.3	94.3	99.4	590	570	3.5
Sp1/7	64.2	96.5	1.23	3.34	13.0	30.5	54.7	98.3	99.7	589	567	3.6
Sp1/6	51.3	87.9	1.55	3.91	15.2	39.2	66.7	98.8	99.8	577	556	3.6
Sp1/5	66.6	96.5	1.07	1.93	10.7	26.4	53.1	98.2	99.7	550	530	3.7
Sp1/4	26.9	41.7	1.85	3.74	24.9	59.5	87.3	99.95	100	592	569	3.9
Sp1/3	96.9	140.1	0.99	0.90	10.6	24.3	41.9	88.1	98.0	632	610	3.5
Sp1/2	120.5	168.9	0.44	−0.33	6.70	15.6	28.9	82.4	98.2	613	591	3.5
Sp1/1	85.7	116.3	1.08	1.90	10.1	22.3	43.4	93.6	99.1	623	601	3.5
Sp1/0	39.9	72.9	2.13	7.30	22.5	48.6	76.4	99.1	99.7	529	508	4.0
Sp2 Palaeo 3 (upper part)	22.0	6.5	2.76	11.82	34.7	68.3	90.2	99.7	99.98	393	376	4.3
Sp2 Palaeo 2 (middle part)	30.3	41.7	4.35	33.11	24.1	57.9	86.3	99.1	99.6	404	370	8.5
Sp2 Palaeo 1 (lower part)	17.1	4.9	3.02	10.67	49.8	78.6	91.8	99.8	100	323	304	5.9
Sp2/12	77.1	153.8	1.26	1.25	11.5	31.3	56.2	91.2	98.8	527	508	3.5
Sp3B (transition with palaeosol Sp3/1)	33.4	41.7	3.56	24.55	20.1	51.7	83.3	99.4	99.7	560	533	4.9
Sp3A (palaeosol Sp3/1)	14.2	4.9	4.04	20.53	45.9	82.3	95.3	99.8	100	295	276	6.5

Only the fraction below 2 mm was studied for both measurements. See Fig. 6 for the position of the different samples analysed.

migration. Radiocarbon dating performed on two 1-mm-sized charcoal fragments from profile Sp2 yielded ages of cal 3349–3026 BC and cal 3342–3029 BC for the lower and upper parts of the unit, respectively (Fig. 7). The deposition of unit B clearly indicates that a change in sedimentary processes and fluvial geomorphology combined with an increasing sediment accretion rate and river transport capacity occurred during the second half of the mid-Chalcolithic.

Unit C is found above unit B in the Sp1 and Sp2 profiles (Figs. 5 and 7). Grain-size analyses show a modal index of ca. 150–160 µm, while the mean grain-size indicates the presence of sandy silts (ca. 80 µm). Magnetic susceptibility values (Table 3) are situated around $500–550 \times 10^{-8}\ m^3\ kg^{-1}$ and are associated with low χfd (around 3.5%). These results and the field observations suggest that the deposition of unit C occurred in similar conditions to that of unit A, with regular aggradation and low transport capacity. Proximal floodplain facies are dominant (Fig. 7). The lower part of unit C was radiocarbon dated to ca. cal 3328–2918 BC, showing a temporal continuity with unit B. The location of unit C at the top of the sequence provides evidence for a subsequent incision period.

General Stratigraphy of the Profile Sp3

The profile Sp3 is located ca. 250 m downstream from Sp1 and Sp2 (Figs. 4B, 5 and 8). Based on the field observations and laboratory analyses, four sedimentary units (1, 2, 3 and 4; Figs. 3 and 8) can be distinguished from the base to the top (the bedrock has not been recognised):

Unit 1 is up to 3 m thick and composed of coarse pebbles in a grey-white sandy matrix (Fig. 8). The pebbles are predominantly angular (only 10–25% of well-rounded pebbles), and originate from the middle catchment (marls and limestones). No charcoal, organic deposits or human artefacts have been found, preventing the dating of this unit. Unit 1 is different from any of the deposits observed in the Sp1 and Sp2 sequences and seems from the coarser grain-size and different clast composition (petrology) to have been deposited in a torrential flood dominated regime.

Unit 2 is separated from unit 1 by a sharp erosional contact (Fig. 8). This 0.80–1 m thick unit is mainly composed of thin beds (10 cm) of orange clays, rich in white carbonate/gypsum concretions, alternating in the lower part with grey silts. No human artefacts were identified and no radiocarbon dating obtained due to the paucity of organic carbon within the sediments. Unit 2 is also characterised by the presence of a dark layer at the top (Sp3/1, Figs. 5 and 8). This layer is well-preserved along the whole profile with a constant thickness of ca. 0.40 m. Magnetic susceptibility measurements (Table 3) performed on Sp3/1 yielded values ranging from ca. 275 to $535 \times 10^{-8}\ m^3\ kg^{-1}$,

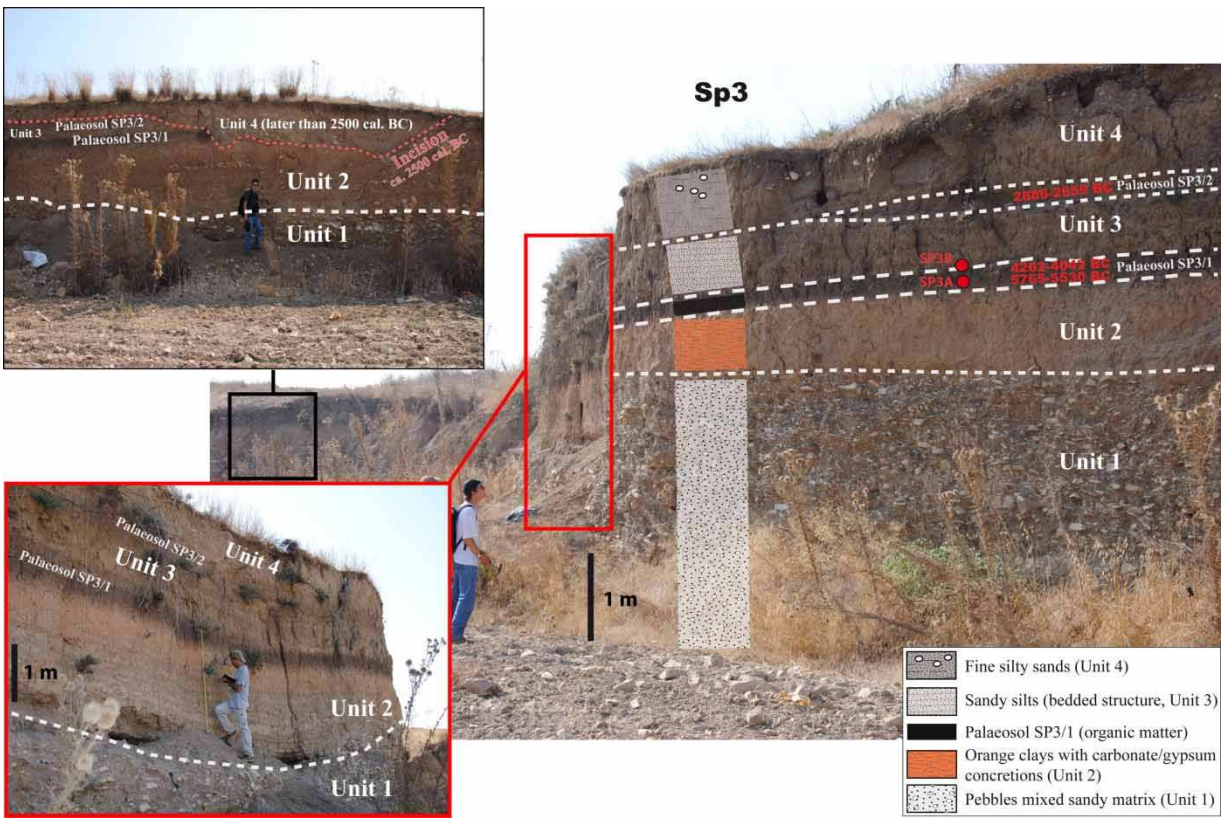

Figure 8 The Sp3 profile showing the Sp3/1 and Sp3/2 palaeosols. Samples from Sp3A and Sp3B were studied for magnetic susceptibility and LASER grain-size measurements (see Table 2 for details).

while χfd measurements yielded high values (between 4.5 and 6.5%, Table 3). This indicates an important contribution of superparamagnetic minerals and is a higher signal than in the catchment sediments (typically ranging between 2.5 and 3.5%, Table 2). It is also suggestive of pedogenic processes. Together with field observations, this result makes it possible to interpret this dark layer (Sp3/1) as a palaeosol. Radiocarbon dating of diffuse organic matter found in the intermediate part of Sp3/1 gave an age of cal 5765–5530 BC while that from the uppermost part (Fig. 8) gave an age of cal 4262–4042 BC. The age range indicates very slow development (approximately 20 cm in ca. 1500 years), mostly during the Late Neolithic.

Unit 3 is found above the palaeosol Sp3/1 and is composed of grey and white silts, alternating with thin beds (5 cm) of white nodules (carbonate concretions). This unit is likely to be associated with quiet fluvial environments with low river transport capacity. The upper part of this last unit is characterised by the presence of a second dark layer (Sp3/2) that does not exceed 0.20 m in thickness and is often eroded, in contrast to Sp3/1 which is generally well-preserved (except in some sections – e.g. Fig. 8, top left picture). No magnetic measurements have been performed on Sp3/2, but the similarity of facies suggests a pedogenic origin as for palaeosol Sp3/1. A radiocarbon date from the intermediate part of Sp3/2 yielded an age of cal 2886–2659 BC and indicates that a palaeosol developed during Late Chalcolithic times. Radiocarbon ages for unit 3 therefore range from ca. cal 4000 to 3000 BC. This and the nature of the facies suggest that it is equivalent to the uppermost part of unit A from Sp1 and Sp2 (also indicative of a calm and continuous fluvial environment).

Unit 4 is found above unit 3 and palaeosol Sp3/2. The modern soil is developed within it and it is composed of grey silty-sands together with isolated pebbles (probably reworked). Unit 4 is characteristic of quiet fluvial environments locally reworking older material. It is worth noting that unit 4 locally directly overlies unit 3 or the palaeosol Sp3/2 (Fig. 8, top left picture). This irregular transition from unit 3 to unit 4, observed along the Sp3 profile, may indicate that a minor period of erosion occurred after the development of palaeosol Sp3/2.

Discussion

Reconstructing the Palaeogeography of the Lower Tremithos River: Evidence for Regular Fluvial Activity from the Late Neolithic to Late Chalcolithic Times

The three profiles studied (Sp1, Sp2 and Sp3) provide evidence for regular deposition (without any major phase of incision) of predominantly well-sorted fine-grained sediments, associated with a meandering fluvial pattern, between ca. cal 4800 BC (Sotira Neolithic Culture) and ca. cal 2500 BC (Late Chalcolithic). The upper part of the sequence is truncated by post-depositional incision (T3 incision). These results are consistent with research conducted in the Gialias catchment (Devillers and Morhange 2011) suggesting a regional control on fluvial evolution. It is also worth noting that the sequences show no inversion in the radiocarbon-derived chronologies. This suggests direct sediment transfer from the upper catchment to the floodplain, with limited reworking.

Our research suggests a Chalcolithic occupation in the area with the discovery of the characteristic Red Monochrome pottery dated to the mid-Chalcolithic period (ca. cal 3000 BC). The presence of large and intact pottery sherds embedded within the sandy deposits (unit A), and situated below the pebbly layer (unit B), indicates that humans may have settled within the Tremithos. Reworking of the sherds by the river is not likely because there is no evidence of abrasion. The absence of any associated archaeological structures may be a consequence of both the limited outcrop area and/or the use of perishable material during the Chalcolithic for building structures. The associated high χfd values (> to 6%) confirm the presence of a thin palaeosol that probably formed during a limited period of time. Finding a palaeosol associated with this pottery suggests the existence of an ephemeral occupation site. The stratigraphy suggests that humans settled on the floor of Tremithos valley during a period when the water level was lower, ca. cal 3200 BC. This is contemporaneous with the 5.2 ka climate event that is considered in the eastern Mediterranean to be a period of drought (Bar-Matthews *et al.* 1997; Roberts *et al.* 2011). The palaeosol and associated archaeological artefacts were subsequently buried by the deposition of coarse material (unit B, Figs. 3 and 7) originating from the upper catchment (where the fine and coarse fractions are dominated by a high ferromagnetic mineral content). Sudden burial might explain the good state of preservation of the artefact. The deposition of unit B (coarse fluvial material) is also likely to be associated with the more arid conditions that prevailed in the Tremithos catchment during the 5.2 ka event. As recognised in other areas (Boyer *et al.* 2006; Wolf *et al.* 2014), increased aridity was able to modify the vegetation cover, and hence generating strong erosion on the slopes under irregular fluvio-torrential conditions. The debris that gradually accumulated on the valley floors during the 5.2 ka period of water flow reduction could have been subsequently evacuated towards the lower Tremithos as a result of flood events.

A subsequent shift towards wetter conditions seems to be recorded by the deposition of unit C, at the beginning of the third millennium BC (Figs. 7 and 8). This return to wetter conditions after a period of drought (e.g. the 5.2 ka event) is well-recorded elsewhere in the eastern Mediterranean (e.g. Robinson *et al.* 2006).

The deposition of unit C in Sp1 and Sp2 and of unit 3 in Sp3 is followed by incision that can plausibly be dated to ca. cal 2500 BC (Fig. 8, top left picture). Subsequently, a last phase of deposition, later than cal 2500 BC (Figs. 7 and 8), is only recorded at Sp3 (unit 4, Figs. 3A and 7). Finally, a major incision of ca. 8–10 m (T3 incision) occurred in ca. cal 2000 BC (Figs. 7 and 8), but this date remains uncertain due to the lack of sediments dated from this period on the T3 or T2 alluvial terraces. This absence of data also prevents any assessment of the alluvial history of the Bronze Age and later periods and any direct influence of the Tremithos on the palaeoshoreline configuration in the area of Ancient Kition during Hellenistic to Roman times, as suggested by some authors (Morhange *et al.* 2000; Bony 2013).

Proposing a Chronology for the Lower-most Part of the Sp3 Sequence

Due to the lack of age control for the bottom of the Sp3 profile (Fig. 8), the dating of units 1 and 2 remains problematic. Radiocarbon dating in the central part of palaeosol Sp3/1 (at the top of unit 2, see above) yielded an age of ca. cal 5700–5500 BC. Due to the apparently slow palaeosol development at the top of Sp3/1 (20 cm in ca. 1500 years), we assume an age of ca. cal 6200–6000 BC or older for the lower parts of this palaeosol. Therefore, unit 2, consisting of homogeneous orange clays mixed with carbonate concretions (no fluvial facies were identified), could date from any time between the late Glacial period and the early Holocene. If so, the formation of palaeosol Sp3/1 could have been triggered by increased temperature and precipitation following the cold and dry climate conditions that prevailed during the late Glacial period (Casford *et al.* 2002). Unit 1 from Sp3, consisting of heterogeneous material deposited under a high river transport capacity, could then plausibly be associated with flood events during the Pleniglacial or late Glacial periods.

The presence of palaeosols above these assumed late Glacial deposits also sheds new light on the possible palaeo-course of the Tremithos at the Pleistocene–Holocene transition. Some authors have suggested that between the late Glacial and the early Holocene, the Tremithos did not follow its modern course but was aligned further east, towards the Tekke Salt Lake area (Figs. 2 and 3A; Gifford 1978). The chronostratigraphy from the Sp3 profile exhibits two main phases of sediment accumulation separated by a phase of very slow sediment accumulation characterised by orange anoxic clays and white carbonate concretions (sedimentary unit 2, Figs. 3A and 7). This last phase dates approximately from the late Glacial to early Holocene and is not characteristic of any fluvial sediment process. The sediments reflect more the *in situ* chemical alteration of carbonate debris (the decalcification of chalky clays). All this suggests that the Tremithos probably was diverted between ca. 12,000 and ca. cal 7000 BC. One option is the course towards the Tekke Salt Lake, which would be consistent with the observations of Gifford (1978). The cause of this change could be tectonic activity, since the area was subject to constant uplift during the Quaternary. Further investigations to reconstruct both the palaeo river course on the north-western margin of the Tekke Salt Lake and into history of recent tectonic activity is required to resolve this issue.

Factors Controlling the Fluvial Development of the Temithos Valley

Disentangling the different drivers that generated sediment accumulation and incision within the Tremithos catchment during the Holocene is difficult, as confirmed by other research in the eastern Mediterranean (Dusar *et al.* 2011).

The continuous tectonic uplift affecting the southern coast of Cyprus during the late Quaternary (Dalongeville *et al.* 2000) will have provided conditions for incision along the Tremithos river. As noted, the role of tectonics also cannot be excluded to explain the potential channel diversion towards the Tekke Salt Lake during the late Glacial to early Holocene.

Climate is also likely to have directly controlled fluvial dynamics in the stratigraphic profiles reported here; in particular for the main phase of sedimentation in the Tremithos which ranges from the 6th/5th to the 3rd millennium BC. The regular deposition of sedimentary units A and C from Sp1 and 2 and of unit 3 from Sp3 corresponds with humid conditions that prevailed throughout the eastern Mediterranean. The deposition of unit B from Sp1 (coarse and heterogeneous material) seems likely to be associated with environmental stress triggered by the more arid conditions prevailing during the 5.2 ka dry event, facilitating an irregular water regime.

An interesting geoarchaeological aspect that has given the sparse archaeological record in Cyprus for the period from the mid-7th to the mid-6th millennium BC is that our research indicates a major phase of fluvial deposition. This has consequences for taphonomy and could suggest that some sites from the Khirokitia (Neolithic times) and Erimi (Chalcolithic times) periods (Fig. 9) may be buried below fluvial

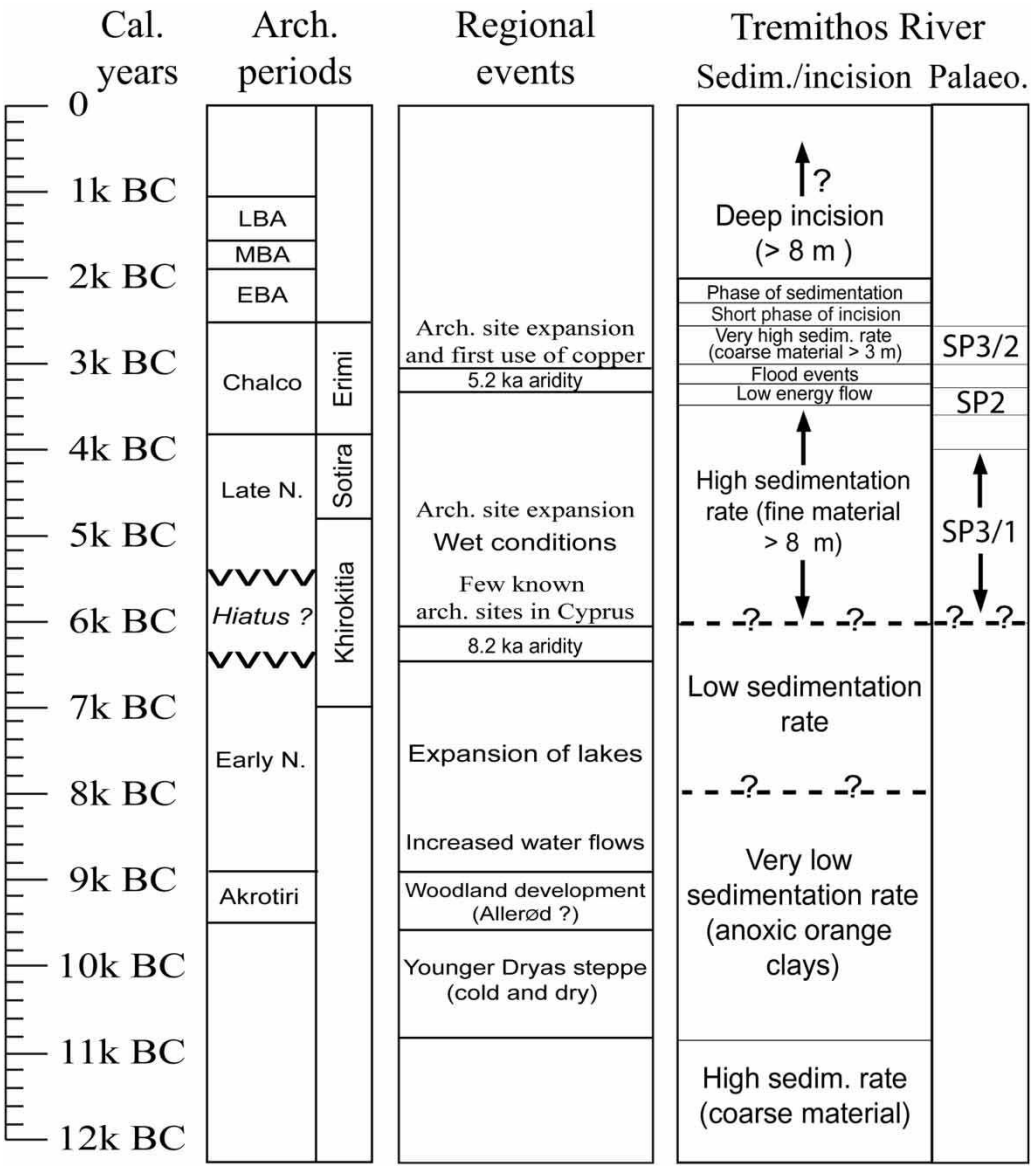

Figure 9 Summary of archaeological periods, regional climate trends and fluvial landscape evolution for the Tremithos basin. Late N.: Late Neolithic; Early N.: Early Neolithic; Chalco: Chalcolithic; EBA: Early Bronze Age; MBA: Middle Bronze Age; LBA: Late Bronze Age; Arch.: Archaeological; Palaeo: Palaeosols; ?: Age uncertainty; Dashed line: proposed chronological limit (with uncertainty); the black arrows indicate the time span.

deposits or hidden by palaeosols. Future archaeological surveys dealing with the Neolithic occupation of the island should consider the possibility of finding evidence for human activity within the thick fluvial terraces of the southern Cypriot rivers rather than limiting research to the rocky promontories as was the case for Khirokitia and Tenta areas.

The evolution of the Tremithos is also likely to have been driven by anthropogenic activity since the mid-Holocene. This study indicates human occupation of the Tremithos catchment during the mid-Chalcolithic period. This period is associated with an increase in human occupation sites across the southern part of Cyprus (Guilaine, 2011). Given the presence of woodland in the upper part of the catchment (Troodos Massif) during the first half of the Holocene (Butzer and Harris 2007), forest clearance for building purposes, or for agriculture, or associated with copper extraction, could have led to periods of intense soil erosion during the Late Chalcolithic and/or early Bronze Age (Butzer and Harris 2007). The transfer of the resulting sediment may also partly explain the rapid accumulation of units B and C from Sp1 and Sp2, which seem to have been deposited in a few centuries. Human influence can also be proposed to explain the incision allocated to the Late Chalcolithic (Knapp *et al.* 1994). This period (ca. cal 2500 BC), which is not characterised by obvious climate change, could potentially be related to major socio-cultural changes (notably different types of agricultural practices and the exploitation of material resources that could affect sediment transfer on the slopes).

A complete Holocene pollen record, coupled with stable isotope analyses (the mostly likely source

being lagoonal sediments), is needed from Cyprus to reconstruct the vegetation history of the area, and help to separate climatic controls on the alluvial history of the Cypriot rivers from anthropogenic impacts.

Conclusion

The study of three stratigraphic profiles has enabled fluvial activity in the Tremithos river (south central Cyprus) to be reconstructed for the first half of the Holocene. Profiles Sp1 and Sp2 provide clear evidence for a phase of more or less continuous sediment accretion from ca. cal 4800 to 2500 BC (the period covering Late Neolithic (Sotira culture) and the Chalcolithic). The Sp3 profile contains a longer sequence than Sp1 and Sp2, possibly ranging from the Pleniglacial to the late 3rd millennium BC. Here, different fluvial environments of deposition have been identified which could mainly be linked to the changing palaeoclimate conditions that directly affected the fluvial pattern of the Tremithos river. Our results also make it possible to assess the role played by climate in the Tremithos valley evolution from the 6th/5th to the 3rd millennium BC when the regular deposition of fine and well-sorted sediments (8 to 10 m thick) associated with a meandering system were recorded. A phase of high-energy deposition of sediments (coarse and heterogeneous material) associated with a braided fluvial pattern (profiles Sp1 and Sp2) is likely to be associated with the 5.2 ka regional dry event. That all the profiles are consistent with the Holocene fluvial reconstructions recently proposed in nearby catchments such as the Gialias suggests a regional climatic control on the dynamics of the river. Further research is however required to unravel the history of Tremithos valley between the Upper Pleistocene and the early Holocene and for the last four millennia, for which period, in this study, deposits from which it would be possible to construct a robust chronostratigraphy were not located.

As for the archaeology, evidence for human activity within the Tremithos catchment is scarce and our investigations did not reveal any Palaeolithic or Neolithic artefacts as might have been expected from the literature. However, our work provides the first indication of human occupation during Chalcolithic (early 3rd millennium BC) with the discovery of a Red Monochrome pottery within fluvial sediments. Additional geoarchaeological studies of the river terraces along the upper river course may well therefore reveal other sites of human occupation within the Tremithos basin.

Acknowledgements

This article is a contribution to the geoarchaeological research programme (FIR, 2010–2012) conducted and directed by Matthieu Ghilardi (CNRS) and Christophe Morhange (University of Aix-Marseille, France) dealing with Holocene landscape changes within the Eastern Mediterranean Islands (Crete, Cyprus and Euboea). This article is also part of the PALEOMEX programme from CNRS (INEE-INSU scientific departments) and was funded by the ARCHEOMED workshop in 2014 (Dirs. Laurent Carozza and Laurent Lespez). The authors would like to thank Dr Sabine Fourrier (UMR HISOMA, CNRS, Lyon, France) for her kind invitation in 2009 to conduct preliminary geomorphological investigations within the Tremithos Valley and for her precious help and assistance during fieldwork. Subsequently, the authors would like to acknowledge Dr Becky Briant (Birkbeck University, London, UK) and Prof David Bridgland (University of Durham, UK) for their fruitful comments and for having improved the English, and two anonymous referees for their comments that helped to improve an earlier version of this manuscript.

References

Bagnall, P. S. 1960. The geology and mineral resources of the Pano Lefkara-Larnaca area. *Geological Survey Department of Cyprus* **5**, 1–116.

Bar-Matthews, M., Ayalon, A. and Kaufman, A. 1997. Late Quaternary paleoclimate in the eastern Mediterranean region from stable isotope analysis of speleothems at Soreq cave, Israel. *Quaternary Research* **47**, 155–68.

Baudou, E. and Engelmark, R. 1983. *The Tremithos valley project. A preliminary report for 1981–1982*. Report of the Department of Antiquities, Cyprus, 1–8.

Baudou, E., Engelmark, R., Niklasson, K. and Wennberg, B. 1985. The Tremithos Valley Project, pp. 369–71 in Papadopoulos, T. and Hadjistyllis, S. A. (eds.), *Acts of the Second International Congress of Cypriot Studies*. Society of Cypriot Studies, Nicosia.

Bintliff, J. 2002. Time, process and catastrophism in the study of Mediterranean alluvial history: a review. *World Archaeology* **33**(3), 417–35.

Bolger, D. 1988. *Erimi-Pamboula. A Chalcolithic Settlement in Cyprus*. British Archaeological, Reports (BAR) International Series 443. Archaeopress Oxford, UK.

Bolger, D., Maguire, L., Quye, A., Kistou, S. and Stephen, F. M. K. 1998. The pottery in Prehistory, pp. 93–147 in Peltenburg, E. (ed.), *Excavations at Kissonerga-Mosphilia, 1979–1992*. Studies in Mediterranean Archaeology, LXX-2, P. Aströms, Jonsered, Göteborg.

Bony, G. 2013. *Contraintes et potentialités naturelles de quelques sites portuaires antiques de Méditerranée et de mer Noire (Fréjus, Ampurias, Orgamé, Kition, Istanbul)*. PhD. thesis, University of Aix-Marseille I, 320 p.

Boyer, P., Roberts, N. and Baird, D. 2006. Holocene environment and settlement on the Çarşamba alluvial fan, south-central Turkey: integrating geoarchaeology and archaeological field survey. *Geoarchaeology* **21**(7), 675–98.

Bridgland, D. and Westaway, R. 2008. Climatically controlled river terrace staircases: a worldwide quaternary phenomenon. *Geomorphology* **98**(3–4), 285–315.

Bronk Ramsey, C. 2009. Bayesian analysis of radiocarbon dates. *Radiocarbon* **51**(1), 337–60.

Brown, A. G. 1985. Late Holocene paleoecology and sedimentary history of a small catchment in central England. *Quaternary Research* **24**(1), 87–102.

Button, S. L. 2010. *Resource Stress and Subsistence Practice in Early Prehistoric Cyprus*. PhD. thesis, University of Michigan, p. 452.

Butzer, K. W. 2005. Environmental history in the Mediterranean world: cross-disciplinary investigation of cause-and-effect for

degradation and soil erosion. *Journal of Archaeological Science* **33**, 1773–800.

Butzer, K. W. and Harris, S. E. 2007. Geoarchaeological approaches to the environmental history of Cyprus: explication and critical evaluation. *Journal of Archaeological Science* **34**, 1932–52.

Buurman, P., Pape, T. and Muggler, C. C. 1996. Laser grain-size determination in soil genetic studies: practical problems. *Soil Science* **162**(3), 211–8.

Casford, J. S. L., Rohling, E. J., Abu-Zied, R. H., Cooke, S., Fontanier, C., Leng, M. and Lykousis, V. 2002. Circulation changes and nutrient concentrations in the late quaternary Aegean Sea: a nonsteady state concept for sapropel formation. *Paleoceanography* **17**, 14.1–14.11.

Collins, P. E. F., Rust, D. J., Bayraktutan, M. S. and Turner, S. D. 2005. Fluvial stratigraphy and palaeoenvironments in the Pasinler Basin, eastern Turkey. *Quaternary International* **140–141**, 121–34.

Dalongeville, R., Bernier, P., Prieur, A. and Champion, T. 2000. Les variations récentes de la ligne de rivage à Chypre. *Gémorphologie: Relief, Processus et Environnement* **1**, 13–20.

Dearing, J. 1999. *Environmental magnetic Susceptibility using the Bartington MS2 System*. Kenilworth: Chi Publishing, p. 104.

Dearing, J. A., Dann, R. J. L., Hay, K., Lees, J. A., Loveland, P. J., Maher Barbara, A. and O'Grady, K. 1996. Frequency-dependent susceptibility measurements of environmental materials. *Geophysical Journal International* **124**(1), 228–40.

Deckers, K. 2002. *Cypriot Archaeological Sites in the Landscape: An Alluvial Geo-Archaeological Approach*. PhD thesis, University of Edinburgh, Edinburgh, p. 340.

Deckers, K. 2003. The Western Cyprus Geoarchaeological Survey: some case-studies, pp. 27–34 in Brysbaert, A., de Bruijn, N., Gibson, E., Michael, A. and Monaghan, M. (eds.) *SOMA 2002. Symposium on Mediterranean Archaeology*. British Archaeological Reports (BAR) International Series 1142. Archaeopress, Oxford, UK.

Deckers, K. 2005. Post-Roman history of river systems in Western Cyprus: causes and archaeological implications. *Journal of Mediterranean Archaeology* **18**, 155–81.

Deckers, K., Sanderson, D. C. W. and Spencer, J. Q. 2005. Thermoluminescence screening of un-diagnostic sherds from stream sediments to obtain a preliminary alluvial chronology: an example from Cyprus. *Geoarchaeology* **20**, 67–77.

De Moor, J., Kasse, C., van Balen, R., Vandenberghe, J. and Wallinga, J. 2008. Human and climate impact on catchment development during the Holocene – Geul river, the Netherlands. *Geomorphology* **98**, 316–39.

Devillers, B. 2005. *Morphogenèse et anthropisation holocènes d'un bassin versant semi-aride : Le Gialias, Chypre*. PhD. thesis, University of Aix Marseille 1, 2 vol., 416 p.

Devillers, B. 2008. *Holocene Morphogenesis and Anthropisation of a Semi-arid Watershed, Gialias River, Cyprus*. British Archaeological Reports (BAR) International Series 1775. Archaeopress, Oxford, UK, 197 p.

Devillers, B. and Morhange, C. 2011. Présentation géomorphologique et potentialités géoarchéologiques du site de Shillourokambos, pp. 1–18 in Guilaine, J., Briois, F. and Vigne, J. D. (eds.), *Un établissement néolithique précéramique à Chypre. Les fouilles du secteur 1*. Athènes: Ecole Française d'Athènes, 17 p.

Devillers, B., Morhange, C., L'Air, M. B. D., Bourcier, M. and Provansal, M. 2002. Détritisme, potentialités et aménagements du territoire à l'Age du Bronze sur les secteurs amont (Potamia-Agios Sozomenos) et aval de Messarée orientale, secteur d'Enkomi-Acheritou) du bassin versant du Gialias (Chypre). *Cahier du Centre d'Étude Chypriotes, Diffusion De Boccard* **32**, 33–52.

Dikaios, P. 1962. *The Swedish Expedition. IV. The Stone Age and the Early Bronze Age in Cyprus*. Lund: The Swedish Cyprus Expedition.

Dusar, B., Verstraeten, G., Notebaert, B. and Bakker, J. 2011. Holocene environmental change and its impact on sediment dynamics in the Eastern Mediterranean. *Earth-Science Reviews* **108**(3), 137–57.

Finné, M., Holmgren, K., Sundqvist, H. S., Weiberg, E. and Lindblom, M. 2011. Climate in the eastern Mediterranean, and adjacent regions, during the past 6000 years – A review. *Journal of Archaeological Science* **38**, 3153–73.

Fuchs, M. 2007. An assessment of human versus climatic impacts on Holocene soil erosion in NE Peloponnese, Greece. *Quaternary Research* **67**, 349–56.

Ghilardi, M. and Boraik, M. 2011. Reconstructing the Holocene depositional environments in the western part of Ancient Karnak temples complex (Egypt): a geoarchaeological approach. *Journal of Archaeological Science* **38**(12), 3204–16.

Ghilardi, M., Kunesch, S., Styllas, M. and Fouache, E. 2008. Reconstruction of Mid-Holocene sedimentary environments in the central part of the Thessaloniki Plain (Greece), based on microfaunal identification, magnetic susceptibility and grain-size analyses. *Geomorphology* **97**(3–4), 617–30.

Gifford, J. A. 1978. *Paleogeography of Archeological Sites of the Larnaca Lowlands, Southeastern Cyprus*. PhD. thesis, University of Minnesota, p. 192.

Gomez, B. 1987. The alluvial terraces and fills of the lower Vasilikos valley, in the vicinity of Kalavasos, Cyprus. *Transaction of the Institute of British Geographers* **12**, 345–59.

Gomez, B. 2003. Alluvial sedimentation and landscape stability, in: M. Rautman (Ed.), A Cypriot Village of Late Antiquity. *Journal of Roman Archaeology Supplementary Series*, vol. 52, 264–6.

Grove, T. 1977. The geography of semi-arid lands. *Philosophical Transaction of the Royal Society London, Series B* **278**, 457–75.

Guilaine, J. 2011. La période Sotira/Chalcolithique ancien, pp. 211–8 in Guilaine, J., Briois, F. and Vigne, J. D. (eds.), *Shillourokambos. Un établissement néolithique précéramique à Chypre. La fouille du Secteur 1*. Editions Errance/Ecole Française d'Athènes. Paris and Athens.

Guilaine, J., Briois, F., Vigne, J. D. and Carrère, I. 1999. Découverte d'un Néolithique précéramique ancien chypriote (fin 9e, début 8e millénaires cal BC), apparenté au PPNB ancien/moyen du Levant Nord. *Comptes Rendus de l'Académie des sciences*, 75–82.

Jordanova, N., Kovacheva, M., Hedley, I. and Kostadinova, M. 2003. On the suitability of baked clay for archaeomagnetic studies as deduced from detailed rock magnetism studies. *Geophysical Journal International* **153**(1), 146–58.

Karageorghis, V. 1982. Chronique des fouilles et des découvertes archéologiques à Chypre en 1981. *Bulletin de Correspondance Hellénique* **106**(2), 685–744.

Kashima, K. 2002. Environmental and climatic changes during the last 20,000 years at Lake Tuz, central Turkey. *Catena* **48**, 3–20.

Kinnaird, T. C., Robertson, A. H. F. and Morris, A. 2011. Timing of uplift of the Troodos Massif (Cyprus) constrained by sedimentary and magnetic polarity evidence. *Journal of the Geological Society* **168**, 457–70.

Knapp, A. B. 2013. *The Archaeology of Cyprus: from Earliest Prehistory through the Bronze Age*. Cambridge University Press, p. 640.

Knapp, A. B., Held, S. O. and Manning, S. W. 1994. The prehistory of Cyprus: problems and prospects. *Journal of World Prehistory* **8**, 377–453.

Le Brun, A., Cluzan, S., Davis, S. J. M., Hansen, J. and Renault-Miskovsky, J. 1987. Le Néolithique précéramique de Chypre. *L'Anthropologie* **91**, 283–316.

Lemcke, G. and Sturm, M. 1997. ^{18}O and trace element measurements as proxy for the reconstruction of climate changes at Lake Van (Turkey): preliminary results, pp. 653–78 in Nüzhet Dalfes, H., Kukla, G. and Weiss, H. (eds.) *Third Millennium B.C. Climate Change and Old World Collapse: NATO ASI Series*. Global Environmental Change, vol. 49. Springer, Berlin.

Lespez, L. 2003. Geomorphic responses to long-term land use changes in Eastern Macedonia (Greece). *Catena* **51**(3–4), 181–208.

Marchetto, A., Colombaroli, D. and Tinner, W. 2008. Diatom response to Mid-Holocene climate change in Lago di Massaciuccoli (Tuscany, Italy). *Journal of Palaeolimnology* **40**, 235–45.

Mayewski, P. A., Rohling, E. J., Stager, J. C., Karlen, W., Maasch, K. A., Meeker, L. D., Meyerson, E. A., Gasse, F., van Kreveld, S., Holmgren, K., Lee-Thorp, J., Rosqvist, G., Rack, F., Staubwasser, M., Schneider, R. R. and Steig, E. 2004. Holocene climate variability. *Quaternary Research* **62**, 243–55.

Morhange, C., Goiran, J. P., Bourcier, M., Carbonel, P., Le Campion, J., Rouchy, J. M. and Yon, M. 2000. Recent Holocene Paleo-environmental evolution and coastline changes of Kition, Larnaca, Cyprus, Mediterranean sea. *Marine Geology* **170**, 205–30.

Noller, J. 2009. *The Geomorphology of Cyprus*. Cyprus Geological Survey. Open file report, Nicosia, Cyprus, pp. 269, 48 maps.

Notebaert, B. and Verstraeten, G. 2010. Sensitivity of West and Central European river systems to environmental changes

during the Holocene: a review. *Earth Science Reviews* **103**, 163–82.

Noti, R., van Leeuwen, J. F. N., Colombaroli, D., Vescovi, E., Pasta, S., La Mantia, T. and Tinner, W. 2009. Mid- to late-Holocene vegetation and fire history at Biviere di Gela, a coastal lake in Southern Sicily, Italy. *Vegetation History and Archaeobotany* **18**, 371–87.

Oberhummer, E. 1903. *Die Insel Cypern: eine Landeskunde auf historischer Grundlage*. Munich, H. (ed.), T. Ackermann, Munchen, Germany, p. 488.

Oldfield, F. 2007. Sources of fine-grained magnetic minerals in sediments: a problem revisited. *The Holocene* **17**(8), 1265–71.

Oldfield, F. and Crowther, J. 2007. Establishing fire incidence in temperate soils using magnetic measurements. *Palaeogeography, Palaeoclimatology, Palaeoecology* **249**, 362–9.

Poole, A. J., Shimmield, G. B. and Robertson, A. H. F. 1990. Late Quaternary uplift of the Troodos ophiolite, Cyprus: Uranium-series dating of Pleistocene coral. *Geology* **18**(9), 894–7.

Reimer, P. J., Bard, E., Bayliss, A., Beck, J. W., Blackwell, P. G., Bronk Ramsey, C., Buck, C. E., Cheng, H., Edwards, R. L., Friedrich, M., Grootes, P. M., Guilderson, T. P., Haflidason, H., Hajdas, I., Hatté, C., Heaton, T. J., Hogg, A. G., Hughen, K. A., Kaiser, K. F., Kromer, B., Manning, S. W., Niu, M., Reimer, R. W., Richards, D. A., Scott, E. M., Southon, J. R., Turney, C. S. M. and van der Plicht, J. 2013. IntCal13 and MARINE13 radiocarbon age calibration curves 0–50,000 years cal. BP. *Radiocarbon* **55**(4), 1869–87. DOI: 10.2458/azu_js_rc.55.16947.

Roberts, N., Stevenson, T., Davis, B., Cheddadi, R., Brewster, S. and Rosen, A. 2004. Holocene climate, environmental and cultural change in the circum-Mediterranean region, pp. 343–632 in Battarbee, R. W., Gasse, F. and Stickley, C. E. (eds.) *Past Climate Variability through Europe and Africa*. Springer, Dordrecht, The Netherlands

Roberts, N., Eastwood, W. J., Kuzucuoglu, K., Fiorentino, G. and Caracuta, V. 2011. Climatic, vegetation and cultural change in the eastern Mediterranean during the mid-Holocene environmental transition. *The Holocene* **21**(1), 147–62.

Robinson, S. A., Black, S., Sellwood, B. W. and Valdes, P. J. 2006. A review of palaeoclimates and palaeoenvironments in the Levant and Eastern Mediterranean from 25,000 to 5000 years BP: setting the environmental background for the evolution of human civilisation. *Quaternary Science Reviews* **25**, 1517–41.

Simmons, A. H. 1999. *Faunal Extinction in an Island society. Pigmy Hippopotamus Hunters of Cyprus*. Springer, New York, p. 381.

Smith, J. P. 1985. *Mineral Magnetic Studies on two Shropshire-Cheshire Meres*. PhD. thesis, University of Liverpool, p. 214.

Todd, I. A. 1987. Vasilikos Valley Project 6: Excavations at Kalavasos Tenta. *Studies in Mediterranean Archaeology*, **71**, 199. Paul Astroms Forlag, Goteborg (Sweden).

Unkel, I., Schimmelman, A., Shriner, C., Forsén, J., Heymann, C. and Brückner, H. 2014. The environmental history of the last 6500 years in the Asea Valley (Peloponnese, Greece) and its linkage to the local archaeological record. *Zeitschrift für Geomorphologie* **58**(2), 89–107.

Vita-Finzi, C. 1969. *The Mediterranean Valleys. Geological Changes in Historical Times*. Cambridge University Press, Cambridge, p. 169.

Vita-Finzi, C. 1993. Evaluating Late Quaternary uplift in Greece and Cyprus. *Geological Society*, London, Special Publications, **76**, 417–24.

Walden, J. and Slattery, M. 1993. Verification of a simple gravity technique for separation of particle size fractions suitable for mineral magnetic analysis. *Earth Surface Processes and Landforms* **18**, 829–33.

Weninger, B., Allam-Stern, P., Bauer, E., Clare, E., Danzeglocke, U., Joris, C., Kubatzki, C., Rollefson, G., Todorova, H. and van Andel, T. 2006. Climate forcing due to the 8200 cal BP event observed at Early Neolithic sites in the Eastern Mediterranean. *Quaternary Research* **66**, 401–20.

Wolf, D., Seim, A. and Faust, D. 2014. Fluvial system response to external forcing and human impact – Late Pleistocene and Holocene fluvial dynamics of the lower Guadalete River in western Andalucía (Spain). *Boreas* **43**(2), 422–49.